INFLUENCE OF STOICHIOMETRY ON ELECTROCHROMIC CERIUM-TITANIUM OXIDE COMPOUNDS

K. von Rottkay, T. Richardson, M. Rubin, J. Slack
Lawrence Berkeley National Laboratory, University Of California, Berkeley, CA 94720, USA,
KvonRottkay@lbl.gov
L. Kullman
Uppsala University, S-75121 Uppsala, Sweden

Abstract

CeO_2-TiO_2 finds use as passive counter-electrode in electrochromic devices. Thin films were produced by dc-sputtering in a wide range of compositions. Influence of total pressure and oxygen partial pressure on the optical constants of TiO_2 was investigated. Slightly substoichiometric TiO_2 films exhibit a red-shift of the bandgap. The TiO_2 content in the compound essentially determines the degree of cathodical coloring upon Li^+ intercalation [1]. However, pure TiO_2 films with comparable visible transmittance in the clear state behave differently during electrochemical cycling depending on oxygen stoichiometry. Films that are deposited at higher total pressure are more oxygen rich and require initial formatting until current voltage cycles become stable. CeO_2-TiO_2 films of intermediate compositions have the relatively highest charge capacity. Comparison with atomic force microscopy indicates a correlation of small grain size with high charge capacity.

Keywords: electrochromic cerium titanium oxide, optical constants, TiO_2, bandgap, grain size, charge capacity, rms roughness

Introduction

CeO_2-TiO_2 finds use as optically passive counter-electrode in electrochromic devices. Optically passive means that the change in visible transmittance upon ion intercalation does not exceed a few percent. Pure TiO_2 itself is known to be cathodically coloring upon ion insertion. Since CeO_2 is only slightly cathodically coloring the TiO_2 content in the compound essentially determines the degree of coloration upon Li^+ intercalation [1].

Experimental

Films were co-deposited by dc-magnetron reactive sputtering using Ti (99.9%) and Ce (99.9%) targets. The Ar (99.9995%) flow rate was varied between 100-220 sccm. O_2 (99.998%)/Ar ratio was varied between 2% and 9%. Deposition pressure ranged from 12 to 36 mTorr, this variation achieved by throttling the turbo pump gate valve. The typical base pressure was below 2.0×10^{-6} Torr. Two or three sputter sources inclined about 20 degrees off normal to a common focal point were used for co-deposition, with a target-to-substrate distance of 17 and 13 cm respectively. Compositional variation was achieved by varying power to each gun between 33 and 520 W. Low Ce content films were easily achieved as the Ce deposition rate per Watt (nm/sW) at 35 W gun power was only 3% of the rate per Watt at 307 W. This disproportionate decrease in rate as Ce power declined is presumably a function of surface oxidation of the target, and was most pronounced at power levels below 90 W.

Films were deposited on In_2O_3:Sn (ITO) glass and fused silica substrates. Prior to deposition the substrate holder was heated to 120°C with the intention of driving moisture from the substrate surface. Deposition began after the holder had cooled to approximately 50°C. The deposition process maintained the temperature at approximately 50°C for the duration of the run. Film thickness ranged from 170 nm to 510 nm as was determined by step-profilometry and ellipsometry.

Optical measurements were made with a variable-angle spectroscopic ellipsometer (VASE) from 280 nm to 1700 nm using an instrument from the J. A. Woollam Co.. Ellipsometric data was taken at three different angles in order to provide data with good signal to noise ratio at each wavelength as well as to over-determine the system of unknown model parameters. To extend the covered spectral range to the whole solar spectrum, transmittance and reflectance measurements from 250 nm to 2500 nm were added; these measurements were taken at near-normal incidence on a Perkin-Elmer Lambda 19 spectrophotometer. The substrate backside was not roughened for ellipsometry to allow later in-situ transmittance control during electrochemical current -voltage cycling. Therefore backside reflections had to be accounted for in the optical model used to extract the optical constants.

Films were tested by cyclic voltammetry in 1M $LiClO_4$/propylene carbonate electrolyte at 1 mV/s over the range 1.8 to 4.0 V using lithium foil for both reference and counter electrodes. The optical transmittance of the films in the visible range was monitored during testing.

Composition and thickness of the samples were characterized by Rutherford backscattering spectrometry (RBS) using a 1.95 MeV $^4He^+$ beam in the 165° backscattering geometry. In addition X-ray Photoelectron Spectroscopy (XPS) was used to determine the Ti/O ratio due to its higher sensitivity to light elements. The XPS measurements were performed with PHI Photoelectron Spectrometer system.. This system includes a hemispherical electron analyzer, an UHV system and a standard Mg K_α source.

Surface morphology was investigated by atomic force microscopy (AFM). Measurements were performed on a Park Scientific M5 instrument. Typical scans were taken over 2 x 2 μm at scan frequencies of 1 Hz. A 0.6 μm Si tip was operated at repulsive forces between 10 and 100 nN in contact mode. Whole images were corrected for slope in fast and slow scan directions and analyzed without filtering.

Results

Optical data was fitted to a structural model containing a parametric dispersion layer for the metal oxide layer and a surface layer simulating the effect of roughness. Details were described in an earlier paper [2]. Fig.1.a,b,c shows the excellent agreement between calculated and experimental data for a TiO_2 film on fused silica substrate. For better readability only every fifth calculated data point is shown.

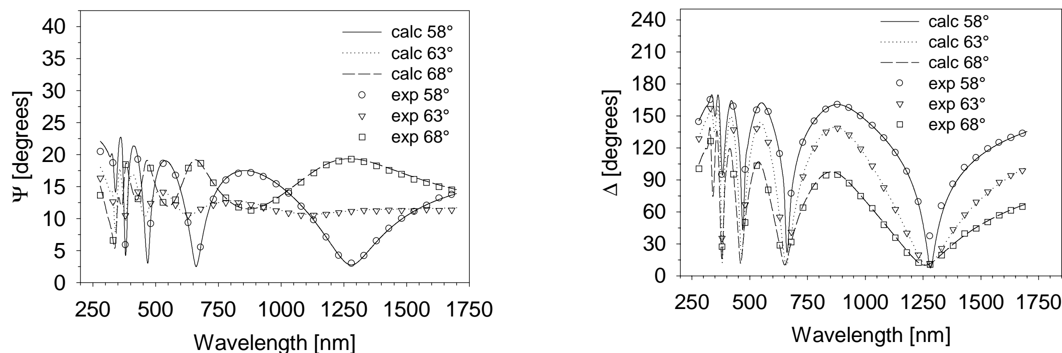

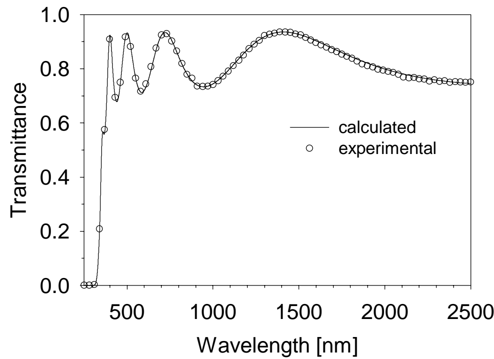

Fig.1a) Fit on ellipsometric Ψ- and 1b) Δ-data and 1c) transmittance data of TiO_2 on fused silica

The spectral refractive index of TiO_2 is a sensitive function of deposition conditions [3-12]. Fig.2a,b shows the optical constants from 0.5 to 5 eV (corresponding to 2500-250 nm) of TiO_2 films grown at different chamber pressures. They decrease when the deposition total pressure increases. This is mainly due to decreasing film density. Due to the increased mean free path at low total pressures the ejected titanium atoms undergo less collisions with other particles before they hit the target. At equal sputtering power the energy of the sputtered titanium atoms arriving at the substrate is therefore higher at lower pressures. This leads to a more compact film structure.

Note the different scale for real and imaginary parts of the refractive index in Fig.2a,b. The extinction coefficient of TiO_2 is zero below 3 eV thus rendering the films transparent throughout the visible spectrum. Our 400 nm thick TiO_2 films on ITO substrate usually have a visible transmittance of 80%. The optical constants for mixed CeO_2-TiO_2 compounds were reported recently [1].

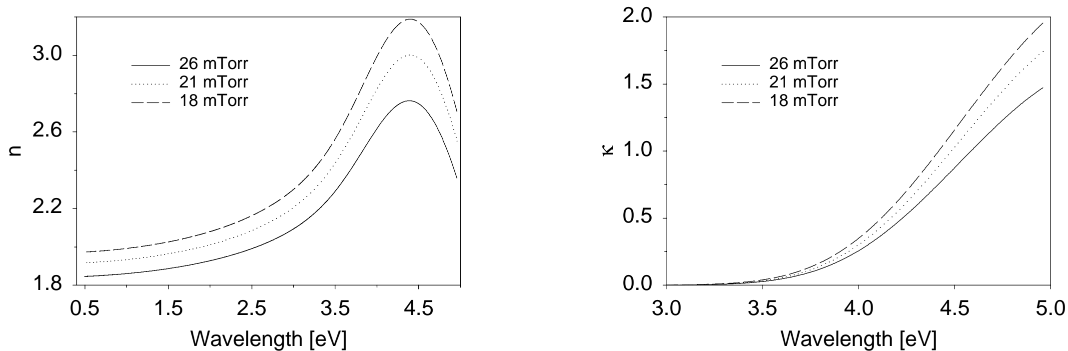

Fig.2a) Real and 2b) imaginary parts of the refractive index of TiO_2 as a function of deposition total pressure

To accurately measure the bandgap of TiO_2 films were deposited on fused silica substrates. Those kind of substrates do not only simplify the structural optical model for the fits over the usual ITO coated glass substrate, but they also exhibit an energetically higher absorption edge. To use substrates other than ITO

coated glass for extracting the bandgap is legitimate since only a comparison of bandgap energies is made. To transfer absolute values to films deposited on ITO one may have to consider differences in thermal expansion coefficients and influence of surface roughness.

The bandgap was determined by from the absorption coefficient assuming an indirect allowed transition [13]:

$$(E - E_g) \propto \sqrt{(E \cdot \alpha)},$$

where E is the energy, E_g is the bandgap energy and α is the absorption coefficient.

A weak red-shift of the bandgap was observed for films deposited at low total pressure (E_g being 3.35 eV at 12 mTorr versus 3.42 eV at 36 mTorr). This is in agreement with a smaller lattice parameter of a more compact film structure.

TiO_2 was also deposited at varying oxygen partial pressures. The bandgap slightly increases as a function of oxygen partial pressure. The behavior is observable in the high-energy end of transmittance spectra [Fig.3.a]. Fig.3.b shows values for E_g that were determined by extrapolating $\sqrt{(E \cdot \alpha)}$ from the regime of linear proportionality to lower energies. The bandgap energies found are in good agreement with reported values for amorphous TiO_2 that lie around 3.4 eV [14-19].

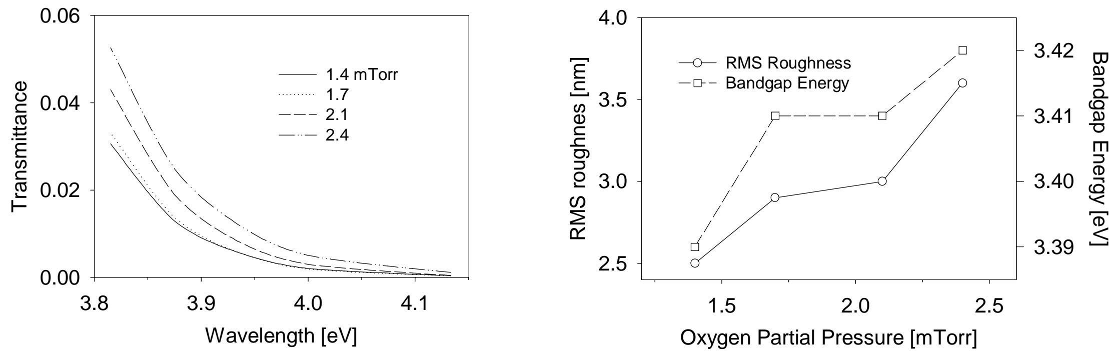

Fig.3a) Transmittance of TiO_2 on fused silica at the absorption edge; 3b) Bandgap energy and rms roughness of TiO_2 as a function of deposition oxygen partial pressure

AFM measurements showed an increasing surface roughness with higher oxygen partial pressure [Fig.3.b]. Results on roughness are taken from films on fused silica deposited at 36 mTorr. Feature size was about 50 nm. Mixed CeO_2-TiO_2 films interestingly showed the root-mean-square roughness δ_{rms} to be lower for intermediate compositions than for the pure components. This could hint to a more pronounced amorphous character in the compound material. Fig.4.a,b,c,d show AFM scans of CeO_2-TiO_2 grown at 25 mTorr on ITO. The typical feature size varies from about 100 nm for the mixed compounds to about 150 nm for the pure components.

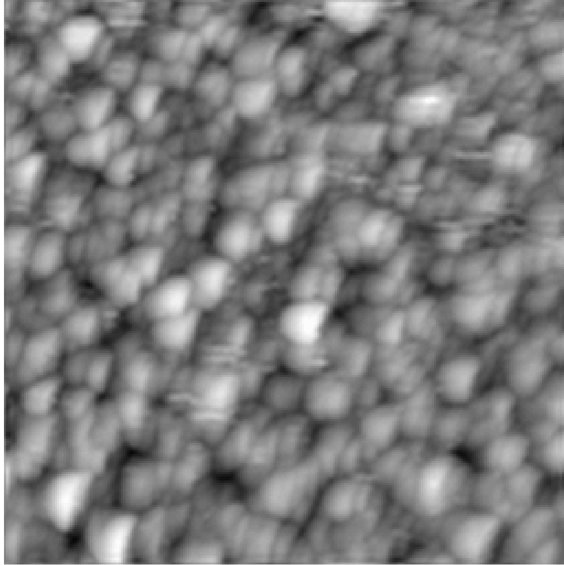

a) CeO_2, $\delta_{rms} = 4.0$ nm

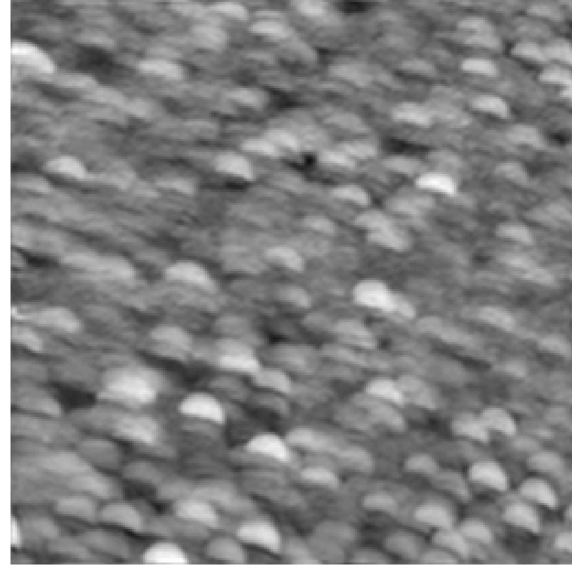

b) $(CeO_2)_{0.67}$-$(TiO_2)_{0.33}$, $\delta_{rms} = 1.4$ nm

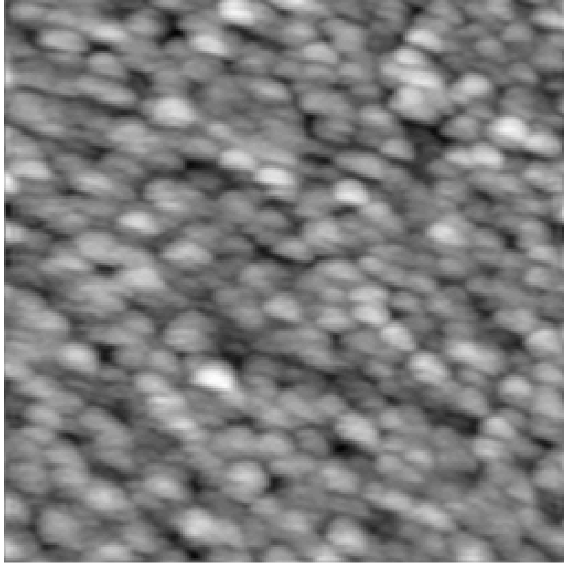

c) $(CeO_2)_{0.44}$-$(TiO_2)_{0.56}$, $\delta_{rms} = 1.2$ nm

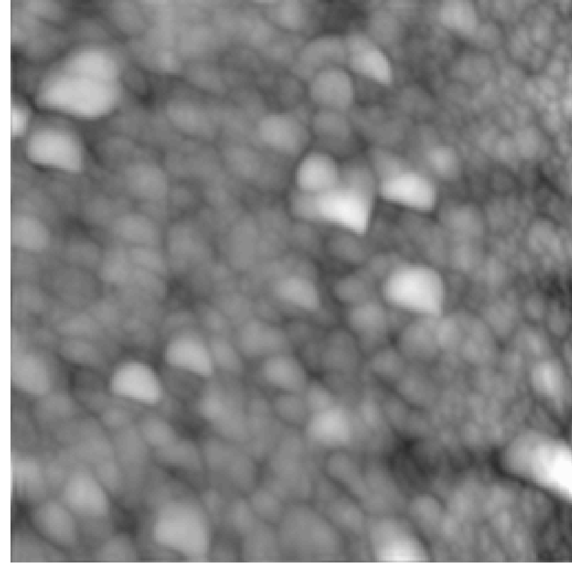

d) TiO_2, $\delta_{rms} = 3.8$ nm

Fig. 4.a,b,c,d) 2x2 μm AFM scans on CeO_2-TiO_2 deposited on ITO in different compositions, rms roughness δ_{rms} is indicated below each picture

The charge capacity of CeO_2-TiO_2 films as a function of cerium content shows that it is higher for intermediate compositions [Fig.5]. From AFM results we know the grain size to be smaller for these films. Therefore the increased Li^+ ion uptake might be explained by grain boundary assisted diffusion: A higher number of grain boundaries will facilitate ion intercalation.

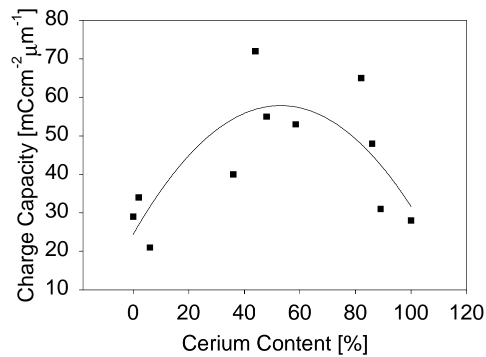

Fig.5) Charge capacity of CeO_2-TiO_2 as a function of cerium content: Ce/(Ce+Ti)[%]

Rutherford backscattering revealed a relative decrease in oxygen content of TiO_2 films grown at low pressures. No absolute values could be obtained for the oxygen content due to the technique's reduced energy selectivity to light elements. However, there seems to be a general oxygen super-stoichiometry due to contamination of the films with carbonates that were identified by XPS measurements, and most likely by water.

Films with comparable visible transmittance can behave differently during electrochemical cycling. Reversible switching of over 70% transmittance was observed for a 470 nm thick TiO_2 film grown at18 mTorr with a 4.5% O_2/Ar gas flow ratio. The coloration efficiency in the visible is 23 cm^2/C.

Films that were deposited at higher total pressure required initial formatting until current-voltage (C-V) cycles became stable. Formatting consisted of an irreversible Li^+ uptake over the first cycles. As those films are more contaminated (by water and other elements present in the chamber) than the low pressure films a possible reason for the initial irreversible Li^+ uptake is the increased amount of oxygen present in the films.

After formatting, coloration efficiency became about 23 cm^2/C for those TiO_2 films, too.

Conclusions

The optical constants of TiO_2 were seen to decrease substantially as a function of total pressure. Films grown at higher pressures are less dense and contain more oxygen mainly due to higher contamination levels. The bandgap of TiO_2 increases with higher total pressure as well as with higher oxygen partial pressures. Bandgap energies for reactively sputtered TiO_2 films on fused silica lie around 3.4 eV.

AFM measurements on CeO_2-TiO_2 films revealed a smaller feature size in mixed CeO_2-TiO_2 than for the components CeO_2 and TiO_2. This effect is clearly visible in the smaller rms roughness. The intermediate films were also found to have a higher charge capacity for Li^+ intercalation. Together this may indicate a grain boundary assisted ion diffusion.

Electrochemical cycling of TiO_2 showed films with higher oxygen stoichiometry to require initial formatting until current voltage cycles became stable. After that the coloration efficiency of 23 cm^2/C compared to TiO_2 with lower oxygen content.

Acknowledgments

This work was supported by the Assistant Secretary for Energy Efficiency and Renewable Energy, Office of Building Technology, State and Community Programs (BTS), Office of Building Systems of the U.S. Department of Energy under Contract No. DE-AC03-76SF00098.

The help of R. Roth with the XPS measurements is thankfully acknowledged.

References

[1] K. von Rottkay, T. Richardson, M. Rubin, J. Slack, E. Masetti, G. Dautzenberg, SPIE Proceedings, Vol.3138 (1997) 9

[2] K. von Rottkay, M. Rubin, S.-J. Wen, Thin Solid Films, 306 (1997) 10

[3] H. K. Pulker, G. Paesold, E. Ritter, Applied Optics 15, (1976) 2986

[4] H. Küster, J. Ebert, Thin Solid Films, 70 (1980) 43

[5] S. Y. Kim, Applied Optics, 35 (1996) 6703

[6] M. Gilo, N. Croitoru, Thin Solid Films, 283 (1996) 84

[7] K. Bange, C. Ottermann, O. Anderson, U. Jeschkowski, M. Laube . R. Feile, Thin Solid Films, 197 (199) 279

[8] C. Ottermann, K. Bange, W. Wagner, M. Laube, F. Rauch, Surf. Interface Anal., 19 (1992) 435

[9] M. H. Suhail, G. M. Rao , S. Mohan, J. Appl. Phys, 71 (1992) 1421

[10] J.-S. Chen, S. Chao, J.-S. Kao, H. Niu, C.-H. Chen, Appl. Optics, 35 (1996) 90

[11] H.-W. Zhang, S.-X. Liu, Thin Solid Films, 209 (1992) 148

[12] G. Atanassov, R. Thielsch, D. Popov, Thin Solid Films, 223 (1993) 288

[13] F. Wooten, "Optical Properties of Solids", Academic Press, New York, 1981

[14] H. Noda, K. Oikawa, T. Ogata, K. Matsuki, H.Kamada, Nippon Kagaku Kaishi (1986) 1084

[15] K.M. Glassford, J.R. Chelikowsky, Phys. Rev. B 45 (1992) 3874

[16] K.M. Glassford, J.R. Chelikowsky, Phys. Rev. B 46 (1992) 1284

[17] J.W. Halley, M.T. Michalewicz, N. Tit, Phys. Rev. B 41 (1990) 10165

[18] J.C. Parlebas, Phys. Stat. Sol. B 178 (1993) 9

[19] B. Poumellec, P.J. Durham, G.Y. Guo, J. Phys. Condens. Mat. 3 (1991) 8195